

Application of machine learning in the determination of rock brittleness for CO₂ geosequestration.

AMINAHO, E.N., HOSSAIN, M., FAISAL, N.H. and SANAE, R.

2025

© 2025 The Authors. Published by Elsevier Ltd. This is an open access article under the CC BY-NC-ND license (<https://creativecommons.org/licenses/by-nc-nd/4.0/>).



Application of machine learning in the determination of rock brittleness for CO₂ geosequestration

Efenwengbe Nicholas Aminaho^{a,b,d,*}, Mamdud Hossain^a, Nadimul Haque Faisal^a, Reza Sanaee^c

^a Robert Gordon University, School of Engineering, Aberdeen, United Kingdom

^b FUTEC Engineering Limited, Glasgow, United Kingdom

^c COWI UK Ltd, United Kingdom

^d A-Class Academic Consults Limited, Port Harcourt, Rivers State, Nigeria

ARTICLE INFO

Keywords:

Geosequestration
Formations
Brittleness
Algorithm
Artificial Neural Network
Concentration

ABSTRACT

The underground storage of carbon dioxide (CO₂), also called CO₂ geosequestration, represents one of the most promising options for reducing greenhouse gases in the atmosphere. However, fluid-rock interactions in reservoir and cap rocks before and during CO₂ geosequestration alter their mineralogical composition, and consequently, their brittleness index which is paramount in determining the suitability of formations for CO₂ geosequestration. Therefore, it is important to monitor the brittleness of reservoir and cap rocks, to ascertain their integrity for CO₂ storage. In this study, an algorithm was developed to generate numerical simulation datasets for a more reliable machine learning model development, and an artificial neural network (ANN) model was developed to evaluate the brittleness index of rocks using data from numerical simulations of CO₂ geosequestration in sandstone and carbonate reservoirs, overlain by shale caprock. The model was developed using Python programming language. The model developed in this study predicted the brittleness index of rocks with an R² value greater than 99 %, and mean absolute percentage error (MAPE) <0.6 % on the training, validation, and testing datasets. Hence, the model predicts the brittleness index of rocks with high accuracy. The findings of the study revealed that the geochemical composition of formation fluids is related to the brittleness index of rocks. In terms of feature importance in predicting the brittleness index of rocks, the concentrations of SiO₂ (aq), SO₄²⁻, K⁺, Ca²⁺, and O₂ (aq) have a stronger impact on the brittleness of rocks considered in this study.

1. Introduction

Carbon dioxide (CO₂) geosequestration represents one of the most promising options for reducing atmospheric emissions of CO₂ (Bachu, 2002). It is the storage part of carbon capture, utilisation, and storage (CCUS). CO₂ geosequestration involves the underground injection and storage of CO₂ and has been recommended as a key solution to global climate change caused by anthropogenic gases in the atmosphere (Wei et al., 2015; Klokov et al., 2017; Liu et al., 2020). CO₂ geosequestration is very feasible as CO₂ can be stored underground in salt caverns (or engineered caverns) or porous media (aquifers or depleted petroleum reservoirs), which are available in different parts of the world. However, for long-term storage of CO₂, underground storage in aquifers or depleted petroleum reservoirs is preferable due to the large storage

capacity of gases in aquifers and depleted petroleum reservoirs (Panfilov et al., 2016).

During CO₂ geosequestration, the petrophysical, geochemical, and geomechanical properties of the formations are altered (Li et al., 2022). CO₂-brine-rock interactions during CO₂ geosequestration result in the dissolution and precipitation of minerals, and consequently alter the porosity and permeability (petrophysical properties) of the rock (Xu et al., 2014; Hedayati et al., 2018; Pearce et al., 2019; Aminaho, 2024). AL-Ameri et al. (2014) and Tariq et al. (2018) studied the time-dependent effect of CO₂ geosequestration on the mechanical properties of rocks. Mechanical weakening of the rock increases with duration of CO₂ geosequestration. Alam et al. (2014) found that the impact of supercritical CO₂ injection on geomechanical properties of chalk depends on the carbonate mineral content, as rocks with high

* Corresponding author.

E-mail addresses: e.aminaho@rgu.ac.uk, aminahonicholas@gmail.com (E.N. Aminaho), m.hossain@rgu.ac.uk (M. Hossain), N.H.Faisal@rgu.ac.uk (N.H. Faisal), rese@cowi.com (R. Sanaee).

<https://doi.org/10.1016/j.mlwa.2025.100656>

Received 9 February 2025; Received in revised form 8 April 2025; Accepted 15 April 2025

Available online 28 April 2025

2666-8270/© 2025 The Authors. Published by Elsevier Ltd. This is an open access article under the CC BY-NC-ND license (<http://creativecommons.org/licenses/by-nc-nd/4.0/>).

carbonate content experience significant mechanical weakening due to CO₂ injection, while rocks with low carbonate content experience negligible amount of mechanical weakening. In sandstone and shale rocks, Young's modulus, uniaxial compressive strength and Brazilian tensile strength decrease with co-injection of supercritical CO₂ and brine (Huang et al., 2018; Lyu et al., 2018). But, the tensile fracturing behaviour of sandstone is not significantly affected by gaseous CO₂ in the presence or absence of water (Liu et al., 2014).

However, at high injection pressure, rocks could experience plastic deformation (Masoudi et al., 2011). Thus, the rocks could fail over a certain amount of plastic deformation depending on the level of brittleness of the rocks. Lyu et al. (2018) found that intact CO₂-brine-shale interactions in low-clay shale samples (with a carbonate or calcite content of only 4.4 wt.%, cristobalite content of 2.88 wt.%, quartz content of 55.50 wt.%, feldspar content of 14.57 wt.%, clay content of 5.85 wt.%, and other minerals) decrease the brittleness values. The CO₂-brine solution has a higher effect on the strength and Young's modulus of the shale rocks than on the brittleness. However, Elwegaa et al. (2019) found that in carbonate-rich shale samples (with 81.6 wt.% calcite, 14.2 wt.% calcite, 3.0 wt.% kaolinite, and 1.3 wt.% basanite), the brittleness index increases during CO₂-brine-rock interactions. In other words, the change in the brittleness index of the rocks during CO₂ geosequestration depends on their initial mineralogical composition before CO₂-brine-rock interactions.

To effectively evaluate the brittleness of rocks before and during CO₂ geosequestration, an automated or advanced monitoring technique that integrates numerical simulations with a machine learning approach, which is calibrated with a few experiments, is paramount (Rashidi et al., 2020). Machine learning creates objectivity, reproducibility, and rapidity in predictions, and saves costs and time needed to perform rigorous numerical simulations and experiments when the need to evaluate integrity of reservoir and cap rocks arises (Hood et al., 2018). The application of machine learning in rock engineering and flow through porous media requires the development of a clear workflow that utilizes experimentally or field data validated physics-based numerical simulations (Chen et al., 2018; Wu et al., 2021) to train an emulator (or a machine learning model), which should be able to evaluate and predict output(s) with high accuracy.

Several studies have been conducted to solve some rock engineering problems, by adopting machine learning approaches (Wang et al., 2021). The application of machine learning has been extended to CO₂ geosequestration (Thanh & Lee, 2022; Ibrahim, 2022, 2023; Punnam et al., 2023; Tariq et al., 2023; Ghorayeb et al., 2024; Wang et al., 2024; Mouallem et al., 2024; Pan et al., 2024; Harati et al., 2024; Tillero, 2024). Ibrahim (2022) conducted a study on the application of machine learning for the prediction of coal wettability during CO₂ geosequestration in coal-water-CO₂ system, by developing adaptive neuro-fuzzy inference system (ANFIS) and artificial neural network (ANN). Dataset generated from experiments was used to train and test the models. The input parameters were the coal properties, operating pressure, and temperature. 70 % of the dataset was used to train the model, while the remaining 30 % of the dataset was used for the testing process. The models were validated with a set of unseen data, and the performance of the models were evaluated based on correlation coefficient (R) and the average absolute percent error (AAPE) between the actual and estimated contact angle. Both models predicted the contact angle in the system with correlation coefficient (R) values higher than 0.96 and mean absolute percentage error (MAPE) <7 %. Thus, these models are useful to screen coal formation targets for CO₂ storage.

Furthermore, Tillero (2024) performed a machine learning-based modelling for geologic CO₂ storage in deep saline aquifers, to predict the effectiveness of CO₂ trapping. The input parameters were CO₂ residual saturation, horizontal permeability, vertical to horizontal permeability ratio, porosity, brine salinity, and CO₂ flow rate; while the output parameters were solubility trapping index, residual trapping index, structural trapping index, and injected CO₂vol. The dataset

generated from numerical simulations was used to train and test the artificial neural network model. The performance of the model was assessed using the coefficient of determination (R²) and root mean square error (RMSE). The R² for training and testing was 96 % and 95 % of precision respectively. Similarly, Thanh et al. (2022) adopted knowledge-based machine learning approaches for the prediction of CO₂ storage performance in saline aquifers. They developed three machine learning-based models: random forest (RF), extreme gradient boosting (XGBoost), and support vector regression (SVR) in the study. The XGBoost-based model predicted more accurately (based on higher R² and very low root mean square error) for CO₂ residual and solubility trapping efficiency. Therefore, the model might be effective in predicting the CO₂ trapping index in other saline formations around the world. However, the CO₂ trapping index or CO₂ storage potential might be influenced by the geochemistry of the formation.

The geochemical composition of formation fluids could be useful in predicting the properties of the formation, as the ionic composition of the fluid is based on fluid-rock chemical interactions. Yu et al. (2020) conducted a study on the geochemistry of formation water in carbonate reservoirs in Ordos basin in China. They established statistical relationships between the formation chemical properties and hydrocarbon storage using the Decision tree algorithm of machine learning. The findings of the study revealed that the Na⁺/Cl⁻ ratio, salinity, Mg²⁺/Ca²⁺ ratio, (Cl⁻-Na⁺)/Mg²⁺ ratio, and (HCO₃⁻ - CO₃²⁻)/Ca²⁺ ratio correlate strongly with the gas preservation. The model accurately predicts where to find gas reservoirs in the Ordos basin, leading to improved exploitation of the hydrocarbon. Therefore, this finding could be extended to reservoir-caprock system, to evaluate their brittleness index before and during CO₂ geosequestration.

Previous studies have developed machine learning models to evaluate CO₂-brine-rock interactions. So far, no study has been conducted to evaluate the brittleness of rocks using a machine learning approach. Machine learning models have been applied in the prediction of rock wettability during CO₂ geosequestration (Ibrahim, 2022, 2023; Tariq et al., 2023; Pan et al., 2024), estimation of CO₂-brine interfacial tension (Mouallem et al., 2024), estimation of volumetric fractions of minerals and CO₂ saturation (Wang et al., 2024), prediction of CO₂ trapping index in saline formations (Thanh et al., 2022; Tillero, 2024), prediction of fluid properties (Ghorayeb et al., 2024; Yang et al., 2024), and to establish statistical relationships between the geochemical properties of formation water and hydrocarbon storage in carbonate reservoirs (Yu et al., 2020).

These studies have shown that brine-rock interactions lead to mineral transformation, and the ionic composition of the formation fluid indicates the type of water-rock interactions (dolomitization, illitization, or dissolution) that have taken place (Yu et al., 2020). Therefore, the ionic composition of formation fluid depends on the mineralogical composition of the rock, as the rock minerals are in equilibrium with the formation fluid. Also, the geochemical composition of the formation fluid depends on the in situ temperature and pressure conditions of the formation (Ibrahim, 2022). As the brittleness index of rocks depends on the mineralogical compositions of the rocks, these parameters (formation fluid ionic composition and other fluid properties, as well as the in situ temperature and pressure conditions) might be related to the brittleness index of the rocks. Also, no algorithm has been developed for the generation of numerical simulation datasets for a reliable machine learning model development, to estimate the brittleness index of formations. Hence, in the present study, an algorithm that incorporates the pre-processing and post-processing stages of numerical simulation datasets for a robust and reliable machine learning model development will be developed, and a machine learning model will be developed to predict the brittleness index of rocks based on their geochemical composition and in situ temperature conditions. Therefore, the aim of this study is to develop an algorithm for the prediction of brittleness index of formations and develop a machine learning model to evaluate the brittleness of reservoir and cap rocks before and during CO₂

geosequestration.

2. Theoretical framework

Fluid-rock chemical interaction during CO₂ geosequestration results in variation in the geomechanical, geochemical, and petrophysical properties of the rock. The changes in the properties of the rock could result in variation in the integrity (mainly brittleness, in this study) of the rock. During CO₂ geosequestration, the fluid-rock chemical interaction results in changes in the ionic composition (including H⁺ concentration) of the formation fluid, fluid density, fluid saturations, and porosity and permeability of the formation. Moreover, initially, the rock minerals are in quasi-stable (or nearly steady-state) condition (Zhang et al., 2011). Thus, the ionic composition of the fluid reflects the initial mineral composition of the formation. For instance, a carbonate rock with siderite (FeCO₃) mineral may contain a higher Fe²⁺ concentration compared to a carbonate rock without siderite mineral, due to siderite dissolution as the formation water approaches quasi-stable condition. Also, dolomite dissolution could result in calcite precipitation (due to abundant Ca²⁺ in the formation fluid), while Mg²⁺ in the formation fluid would increase, resulting in precipitation of magnesium-based minerals during CO₂ geosequestration (Zhang et al., 2011). Therefore, the ionic composition of the formation fluid reflects the mineralogical composition of the formation, and consequently influences the mineralogical brittleness index of the formation.

Brittleness is defined as a deficiency of plasticity during material failure (Hou et al., 2018). It is an important characteristic to evaluate the ‘drillability’ and ‘fracability’ of rocks (Lyu et al., 2018). Rocks that are very brittle are easier to drill and fracture, as they do not exhibit significant ductile or plastic behaviour before failure. In other words, the rock terminates by fracture only slightly beyond or at the yield stress (that is, little or no plastic deformation occurs at failure) (Hucka & Das, 1974; Meng et al., 2015). In terms of a reservoir-caprock system for CO₂ storage, it is important for the caprock to be less brittle relative to the reservoir rock during CO₂ geosequestration to minimize the chance of fracturing the caprock and creating pathways for CO₂ leakage to the earth’s surface. Different methods have been proposed for the evaluation of the brittleness of geomaterials, generally referred to as the brittleness index. Different approaches for the evaluation of the brittleness index of rock are based on geochemical and geomechanical evaluation.

The geochemical approach of brittleness index evaluation is mainly the ratio of sum of the weight of brittle minerals (with or without their respective weighting coefficients) to the total weight of the rock minerals (Kang et al., 2020). Since the brittleness index is calculated using the composition (weight fractions) of minerals in the rock, it can be referred to as the mineralogical brittleness index. The geomechanical approach evaluates brittleness index by elastic parameters (elastic modulus and Poisson’s ratio), strength parameters (compressive and tensile strength) of the material, and stress-strain curve analysis (Li, 2022). As the brittleness index is calculated using mechanical properties of the rock, it can be referred to as mechanical brittleness index (Kang et al., 2020). The brittleness index evaluated based on elastic parameters of the material can be determined using static or dynamic elastic modulus and Poisson’s ratio. The dynamic elastic parameters are calculated from the acoustic or ultrasonic wave velocities (compressional or P-wave and shear or S-wave) and bulk density of the material, while the static elastic parameters are measured directly in a deformational experiment (AL-Ameri et al., 2014; Tariq et al., 2018). The static tests are destructive tests, while the dynamic tests are non-destructive tests. The ratio of P to S wave velocities at different axial and lateral stresses ranges between 1.25 and 1.40 (Heidari et al., 2020). The mechanical brittleness index of rocks can also be determined based on the ratio of compressive to tensile strengths of the formations (Meng et al., 2015).

It is important to understand the changes that occur in the elastic and strength parameters of reservoir and cap rocks during injection and

storage of CO₂ in aquifers or depleted oil or gas reservoirs for long-term stability of CO₂ geosequestration (Huang et al., 2020). In a study conducted by Heidari et al. (2020), the uniaxial compressive strength (UCS), Brazilian tensile strength (BTS) and fracture toughness of brine-saturated sandstone increased with increasing NaCl concentration (in the absence of supercritical CO₂), but decreased after supercritical CO₂ injection; while the elastic moduli of brine-supercritical CO₂ co-saturated sandstone were higher relative to brine-saturation condition, unlike the case of the peak strength. CO₂-brine-shale interactions decrease the brittleness index of a low-clay shale rock (Lyu et al., 2018), while CO₂-brine-shale interactions increase the brittleness index of a carbonate-rich shale rock (Elwegaa et al., 2019). CO₂-brine-shale interaction has more effect on the rock’s strength and Young’s modulus than on the brittleness (Lyu et al., 2018). The changes in the mineralogical composition during CO₂ geosequestration might impact the brittleness index of the rock.

The brittleness index of the formation at different times during CO₂ geosequestration could be predicted using the fluid and rock properties, and other operational conditions, without necessarily using the composition (volume or weight fractions) of the minerals. This can be achieved using machine learning-based models for real-time prediction of the brittleness of formations before or during CO₂ geosequestration. Different machine learning regression algorithms can be used to develop such predictive machine learning models, some of them are artificial neural network (ANN), random forest, support vector regression, and decision tree algorithms (Cao et al., 2020; Yu et al., 2020; Ibrahim, 2022; Nyakilla et al., 2022; Thanh et al., 2022; Kolawole et al., 2023). The ANN is very effective for problems with highly non-linear and complex datasets with a large number of variables or features (Kannaiah & Maurya 2023), and could be useful for the evaluation of the brittleness index of rocks before and during CO₂ geosequestration.

3. Artificial neural network (ANN)

A simple ANN can be referred to as a linear model based on brain architecture made up of neurons like that of the human brain, which receive and transmit information to all adjacent neurons after processing (He et al., 2022). The connections between these neurons are defined by weights. ANN model is structured in layers (input, hidden, and output layers), having nodes in one layer connected to nodes in the following layer. The input layer contains the input parameters, while the output layer contains the output parameters. A hidden layer has multiple neurons. There can be multiple hidden layers in an ANN model. The nodes (or neurons) utilize the weights of the connections to learn the dataset and adopt an activation function to pass their signal to the output layer (Kannaiah & Maurya, 2023). In other words, the learning process of ANN model is to adjust the weights (iteratively) between neurons and the bias of each neuron in the way of repeated input and output (a process referred to as model training); thus, making it possess excellent non-linear fitting abilities (He et al., 2022; Yao et al., 2023). So, the weights of a network are initialized and then updated while training the network. The weights can be updated as follows:

$$w_i = w_{i-1} - \alpha \left(\frac{dLoss}{dw_{i-1}} \right) \quad (1)$$

where w_{i-1} and w_i represent the old weight and updated weights, respectively; α is the learning rate, while $dLoss/dw_{i-1}$ represents the derivative of error (or loss function) with respect to weight.

Some parameters that control the performance of the neural network are optimizers, batch size, and epochs. Optimizers are algorithms used to minimize the loss function or error during model training. This is achieved by modifying or changing the weights and learning rate during training. Some common optimizers are root mean square propagation (RMSprop), stochastic gradient descent (SGD), and adaptive moment estimation (Adam). Furthermore, the fitness of the model to the data can

be improved by choosing an optimum number of batch size and epochs. Batch size controls how many observations in the training data that pass through the algorithm at a time, until the entire training data pass through the algorithm in an epoch. Epochs control how many times the entire training data pass through the algorithm during the training process. The model parameters of the network are updated with each epoch (Kannaiah & Maurya, 2023). A fully connected neural network can be referred to as a multi-layer perceptron (Fig. 1).

The input layer takes the input data (x_i). Each node acts like artificial neurons. Each node in every layer (except the output layer) is connected to each node in the subsequent layer. The procedure of the mathematical solution is illustrated in Fig. 2. The input data layer is 'Layer 1', $w^{(1)}$ is the matrix of weights from layer 1 to layer 2, and $a_i^{(2)}$ is the activation on unit i in layer 2. These weights and activations on nodes (or units) also apply when there are multiple hidden layers. In addition, each layer (except the output layer) has a bias unit which is equal to 1. Mathematically, the activations can be expressed as

$$a_1^{(2)} = h(w_{10}^{(1)}x_0 + w_{11}^{(1)}x_1 + w_{12}^{(1)}x_2 + w_{13}^{(1)}x_3) \quad (2)$$

Similarly, $a_2^{(2)}$ and $a_3^{(2)}$ can be generated. The activation function is represented by h , which in this study is a rectified linear unit (ReLU), expressed as

$$h(x) = \max(0, x) \quad (3)$$

The output layer (in this case, layer 3) is mathematically expressed as

$$\hat{y}(w, x) = a_1^3 = h^*(w_{10}^{(2)}a_0^{(2)} + w_{11}^{(2)}a_1^{(2)} + w_{12}^{(2)}a_2^{(2)} + w_{13}^{(2)}a_3^{(2)}) \quad (4)$$

where, $h^*(x)$ is the activation function on the output unit.

4. Methodology

The research design involves the development of an algorithm to generate numerical simulation data to build a reliable machine learning model, and the development of a machine learning model to evaluate the brittleness index of reservoir and cap rocks, using data from numerical simulations.

4.1. Mathematical modelling

The actual brittleness index of the rocks (based on numerical simulation mineral volume fraction outputs and molecular weight and molar volume of the minerals) was calculated using a mathematical model derived by Aminaho and Hossain (2023). The derived model was based on the brittleness index model developed by Kang et al. (2020). The

mineralogical brittleness index model developed by Kang et al. (2020) was validated using field data in their study. Therefore, the model was proven to be reliable. The model derived by Aminaho and Hossain (2023) which is based on molecular weight, molar volume, and volume fraction of the minerals and that of Kang et al. (2020) which is based on the weight or weight fraction of the minerals should give the same result for the same rock at the same condition. The variables in the brittleness index model derived by Aminaho and Hossain (2023) mathematically replace the weight fraction of the minerals.

The mineralogical brittleness index developed by Kang et al. (2020) is given as:

$$BI_{BMod} = \frac{W_Q + 0.49W_F + 0.51W_C + 0.44W_D}{W_T} \quad (5)$$

where W_Q , W_F , W_C , and W_D represent the weights of quartz, feldspar, calcite, and dolomite, respectively; W_T represents the total mineral weight.

Previous studies have evaluated the brittleness index of rocks based on their mechanical properties. A few studies that evaluated the brittleness index of rocks based on the mineralogical composition of rocks were based on weight fraction of the rock minerals (Kang et al., 2020), thereby limiting the evaluation of the brittleness index of rocks from numerical simulations, as some reactive transport geochemical modelling software (such as TOUGHREACT) output volume fraction (not weight fraction) of rock minerals (Xu et al., 2014). The need to determine brittleness index of rocks based on the volume fraction output from geochemical modelling software led to the derivation of a more robust mathematical model to determine the brittleness index of rocks during CO₂ geosequestration (Aminaho & Hossain, 2023).

The output volume fraction of each mineral from the numerical simulation is the volume of mineral divided by volume of medium including porosity (V_{frac}). Thus, the volume of each mineral divided by total volume of solid [part of the rock] is calculated as follows (Xu et al., 2014):

$$f_m = \frac{V_{frac}}{1 - \phi_{med}} \quad (6)$$

where ϕ_{med} represents [current] porosity of the medium (or grid block), and f_m represents the volume of mineral per volume of [the solid part of] the rock.

The mass fraction of composite materials has been calculated to determine their mechanical properties (Ezema et al., 2015) using their densities and volume fractions. Therefore, it is possible to determine the mass fraction of minerals in a rock following a similar approach. The

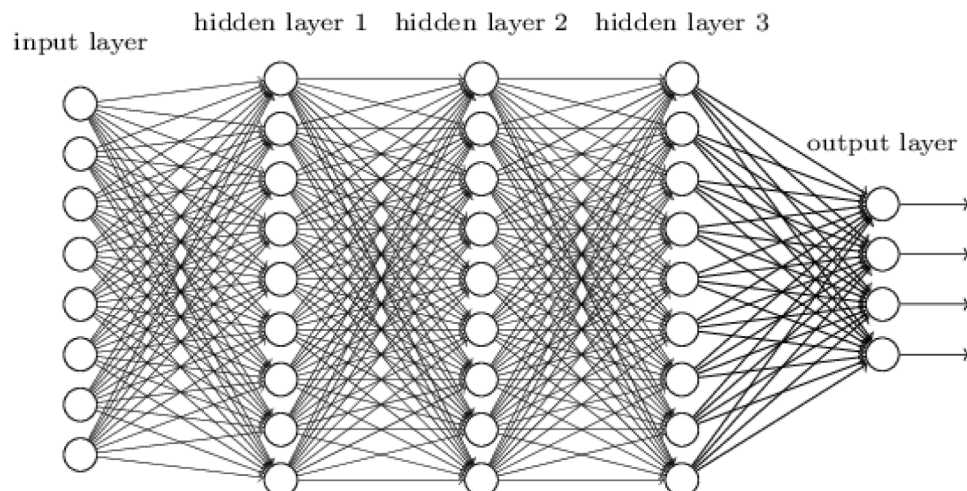


Fig. 1. Fully connected artificial neural network (McNaughton, 2019).

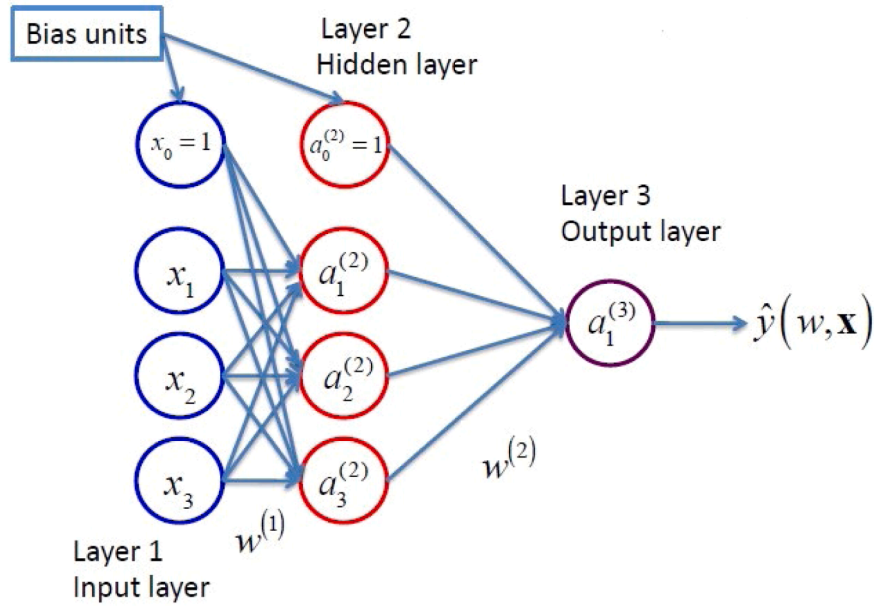


Fig. 2. Demonstration of solution procedure of a fully connected neural network (McNaughton, 2019).

mass fraction of each material that forms a composite structure is the mass of that material to the total mass of the materials that form the structure. Similarly, the mass fraction of each mineral that forms a rock is the mass of each mineral to the total mass of minerals that form the rock, and can be expressed as follows:

$$\begin{aligned} \text{Mass fraction of a mineral, } x_i &= \frac{\text{mass of the mineral,}}{\text{total mass of minerals in the rock,}} \\ &= \frac{m_i}{\sum_{i=1}^{nm} m_i} \end{aligned} \quad (7)$$

$$m = V\rho \quad (8)$$

$$x_i = \frac{v_i \rho_i}{\sum_{i=1}^{nm} v_i \rho_i} \quad (9)$$

where V and ρ represent volume and density of solid, respectively; v_i represents volume fraction of each mineral in the solid part of the rock (same as f_m in Eq. (6)). Density can be expressed as molecular weight divided by molar volume.

$$\rho = \frac{\bar{M}}{\bar{V}} \quad (10)$$

Thus, the mass (or weight) fraction becomes:

$$x_i = \frac{\frac{v_i \bar{M}_i}{\bar{V}_i}}{\sum_{i=1}^{nm} \frac{v_i \bar{M}_i}{\bar{V}_i}} \quad (11)$$

where \bar{M} and \bar{V} represent molecular weight (g/mol) and molar volume (cm³/mol) of mineral. The weight fraction of each of the minerals in the model developed by Kang et al. (2020) can be replaced by x_i . Hence, the mineralogical brittleness index becomes (Aminaho & Hossain, 2023):

$$BI = \frac{\frac{v_Q \bar{M}_Q}{\bar{V}_Q} + \frac{0.49 v_F \bar{M}_F}{\bar{V}_F} + \frac{0.51 v_C \bar{M}_C}{\bar{V}_C} + \frac{0.44 v_D \bar{M}_D}{\bar{V}_D}}{\sum_{i=1}^{nm} \frac{v_i \bar{M}_i}{\bar{V}_i}} \quad (12)$$

4.2. Proposed algorithm for rock brittleness index evaluation in CO₂ storage fields

The determination brittleness index of formations in CO₂ storage fields or sites is very important to ascertain their ductility. Formations with a high brittleness index are less ductile compared to formations with low brittleness index. Highly brittle formations are prone to tensile fracture and initiation (or creation) of cracks. Hence, it is important for reservoirs to have a high brittleness index, while caprock formations should have a low brittleness index for proper containment of the CO₂ in the reservoir and to prevent the migration of CO₂ to the earth's surface. To speed up appraisal of the brittleness index of rocks in CO₂ storage sites, the development of a machine learning model is paramount, using data from numerical simulations.

The application of machine learning for formation brittleness index evaluation will save the time of performing computationally expensive numerical simulations and further data post-processing for brittleness index calculations. The machine learning model would also save the cost of performing expensive laboratory or field experiments to determine the brittleness index of formations before or during CO₂ geo-sequestration. Finally, a machine learning model for rock brittleness index evaluation would enable faster and accurate predictions and better generalization, especially for models trained with wider arrays of datasets from numerical simulations validated using data from several CO₂ storage fields in different parts of the world.

To ascertain the reliability of the numerical simulation data for machine learning model development for brittleness index prediction, an algorithm was developed (Fig. 3) in the present study. The algorithm involves numerical simulation data pre-processing for machine learning model development, and numerical simulation data post-processing for machine learning model development. Stepping through the complete algorithm (pre-processing and post-processing stages) will result in the development of a more robust and reliable machine learning model which can be applied in different CO₂ storage sites or fields.

The pre-processing stage of the algorithm requires a CO₂ geo-sequestration field or experimental design on a laboratory scale, and the design of suitable numerical simulations to model CO₂ storage and migration in porous media. The numerical simulations are performed based on the in situ field temperature and operating pressure conditions, and the rock and fluid properties. The numerical simulations are validated with experimental or field data, ensuring that the mean absolute

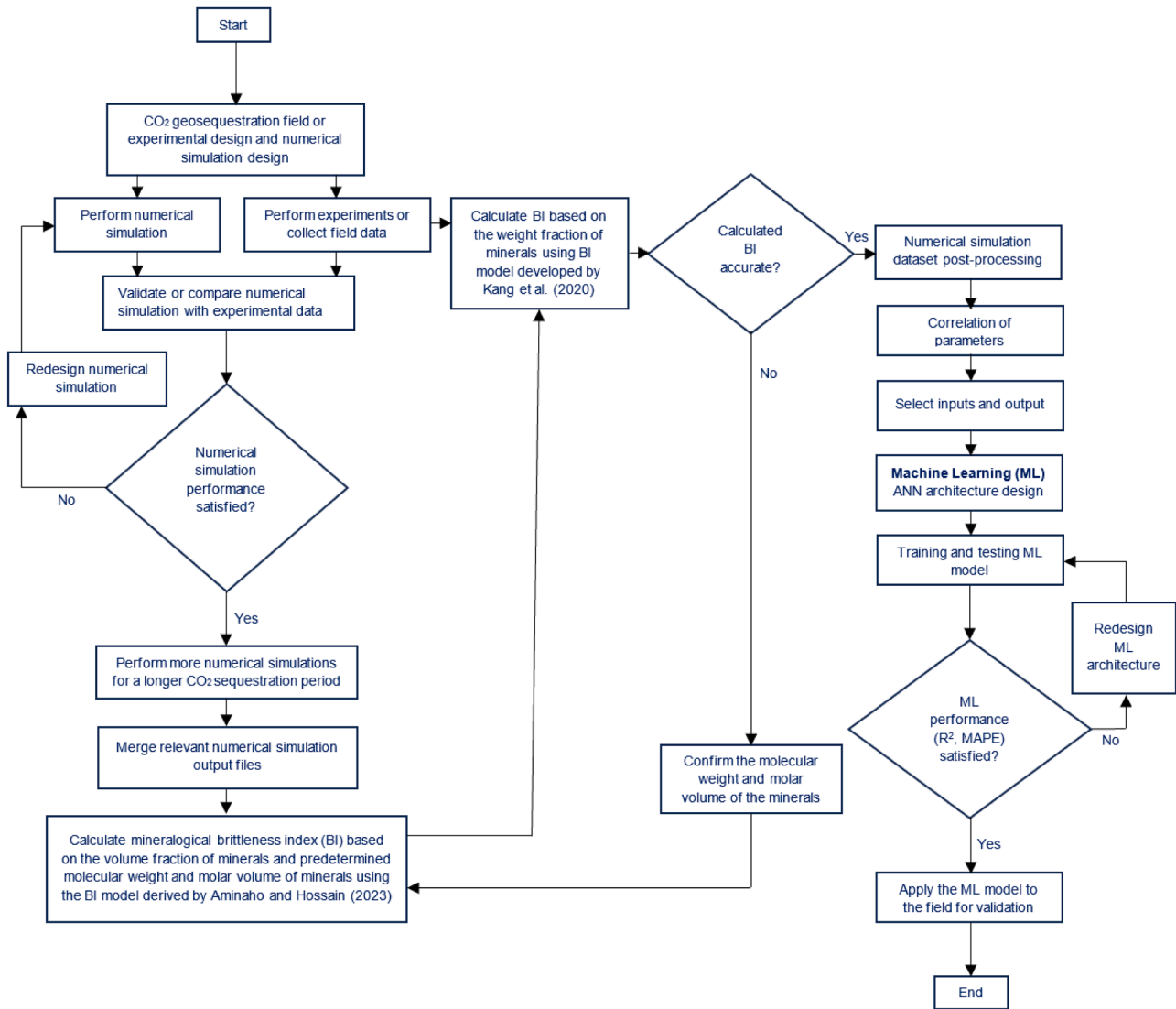


Fig. 3. Proposed algorithm for generating a numerical simulation dataset for reliable machine learning model development to evaluate the brittleness index of formations.

percentage error between the model value and the actual value is within an acceptable limit or the absolute difference (ΔX_i) between the model (numerical simulation) value (X_{i_model}) of the validation parameter (a common variable between the numerical simulation output and the experimental/field data; the common parameter could be the volume fraction of each of the minerals) and the actual (experimental/field) value (X_{i_actual}) of the validation parameter is within the set error limit (ϵ_i); that is $\Delta X_i < \epsilon_i$.

$$\Delta X_i = |X_{i_actual} - X_{i_model}| \quad (13)$$

When the numerical simulation is validated using the experimental and field data, more numerical simulations can be performed, mainly to cover a longer period of CO₂ geosequestration (say, up to 10,000 years), which could not have been possible with laboratory experiments. So, numerical simulations make it possible to evaluate the impact of CO₂ geosequestration on the properties of reservoir and cap rocks during CO₂ geosequestration in hundreds to thousands of years in the future. When the numerical simulations are completed, all relevant simulation output files are merged, and the brittleness index of the formations are calculated (based on the simulation output of volume fraction of the minerals and the molecular weight and molar volume of the minerals which are read from a standard table of previous experiments conducted on

minerals) using the model derived by Aminaho and Hossain (2023). Similarly, from the experimental or field data, the brittleness index of the formations are calculated using the model developed by Kang et al. (2020) based on the weight fractions of the minerals determined by X-ray diffraction (XRD) analyses. The brittleness index calculated from the experimentally validated numerical simulation is expected to be within an acceptable error limit (ϵ_i); otherwise, it is important to confirm that the molecular weight and molar volume of the minerals used in the calculation of the brittleness index based on the numerical simulation are correct. Once the absolute difference between the brittleness index calculated based on the numerical simulation output (volume fraction of the minerals and their molecular weight and molar volume) and the brittleness index calculated using the experimental/field data (weight fraction of the minerals) are within an acceptable error limit, the pre-processing stage of the numerical simulation data is completed, and the post-processing stage of the numerical simulation data can begin.

The post-processing stage commences when the numerical simulations have been validated and the calculated brittleness index is accurate. This implies that the numerical simulation data is possible to be used in the development of the machine learning model. However, before the numerical simulation data is used in building the machine learning model, the dataset is processed further. For example, it is

important to confirm that there are no null values, no missing columns or rows, no duplicated columns or rows, etc. Also at this stage, preliminary statistical analyses are performed to evaluate the type and distribution of the dataset. The correlation coefficients between parameters are determined to identify the relationship between the input parameters and the output parameter(s), and to identify input parameters that are co-correlating with one another (to remove some parameters from the dataset appropriately). At this stage, parameters (input and output) for the machine learning model development are selected. When the parameters are selected a suitable machine learning model and architecture is designed, and the model hyperparameters are tuned to determine the optimum hyperparameters and a suitable machine learning model that predicts the brittleness index of the formations more accurately based on different assessment criteria. The dataset may be divided into training and testing dataset (or training, validation, or testing dataset), and these datasets may be standardised (or normalised) depending on the data distribution or skewness. The machine learning model is trained with the training dataset, and its performance is evaluated with the testing dataset. There are different model performance criteria; some of them are the coefficient of determination (R^2), mean absolute percentage error (MAPE), mean absolute error (MAE), root-mean-square error (RMSE), and mean square error (MSE). The lower the error and the higher the R^2 value, the more accurate the model is. The machine learning model architecture can be adjusted, and the model can be retrained until the model performance becomes acceptable. When the machine learning model performance is acceptable, the model can be validated by testing it with data that has not been seen by the model ('unseen data') to see how well it performs. In this case, the machine learning model can be tested using data from other CO₂ storage sites (or fields) to predict the brittleness index of the formations.

The numerical simulation data used in the machine learning model development in the present study were not validated with experimental or field data, but they were compared using experimental data obtained from AL-Ameri et al. (2016) and Mavhengere et al. (2022). The brittleness index calculations based on data from the numerical simulations could not be validated using rock core samples, as some portion of the fluids injected into the reservoir migrated to the caprock (Aminaho, 2024). Therefore, field data would have been more suitable to validate such numerical simulations. However, no field data with such simulation cases was available at the time of the study. Hence, the machine learning model developed in the present study was based only on the post-processing stage of the numerical simulation dataset.

4.3. A case study of numerical simulation data post-processing for machine learning model development

Machine Learning (ML) is a subset of artificial intelligence that integrates statistics and computer science to build algorithms that become more efficient when they are subject to relevant data instead of giving a specific instruction. Machine learning helps produce predictions or decisions without being specifically produced for the task (Jijo & Abdulazeez, 2021). Machine learning algorithm creates a model population based on a sample called training data, such that test data can be used to test the efficiency or accuracy of the developed model. Among several applications of machine learning, it can be used for classification and regression purposes. In this study, a regression model was developed using an artificial neural network (ANN) algorithm to predict the brittleness index of rocks.

4.3.1. Data preparation

Data from numerical simulations in Strategies 1 and 2 of CO₂ geo-sequestration in the study conducted by Aminaho (2024) were used in developing the machine learning model. The concentration and mineral data from the TOUGHREACT numerical simulation were merged, and data of all the modelled cases (in comma-separated values file format) were concatenated to cover a wide range of data for the model

development, making a total of 38,080 observations (or rows). The mineralogical brittleness index of the formations was calculated for each of the observations using the brittleness index model (the model that considers the bulk modulus of brittle minerals) derived by Aminaho and Hossain (2023) using the volume fraction, molecular weight, and molar volume of the minerals. Thus, a new column for brittleness index was created, making a total of 51 features in the dataset.

In order to create a dataset for the machine learning model development, to predict brittleness index, all the mineral volume fraction columns were deleted (or dropped) to ensure the prediction of the brittleness index is not influenced by the mineral volume fractions from which the brittleness index was calculated. This is because the goal of developing the machine learning model in the present study is to demonstrate how other features can be used to predict the brittleness index of the rocks.

The correlation coefficients between each of the variables with another were determined using the Pearson correlation coefficient (r), expressed as

$$r = \frac{n \sum xy - (\sum x)(\sum y)}{\sqrt{[n \sum x^2 - (\sum x)^2][n \sum y^2 - (\sum y)^2]}} \quad (14)$$

where n is the number of observations, and x and y represent the correlated features.

It is good and acceptable to have a strong correlation between dependent and independent variables. However, it is undesirable to have a strong correlation between two independent variables. When two independent variables strongly correlate with each other, it suggests that excluding one of them from the training data would be beneficial to prevent redundancy and help to improve the model performance (Kannaiah & Maurya, 2023). Hence, for two independent variables in the dataset perfectly correlating ($r = 1.0$) with each other, one of the features is removed. For instance, temperature and pressure, liquid saturation and gas saturation, permeability in the x and z directions, and permeability ratio in the x and z directions, correlate perfectly with each pair. Therefore, one of each feature was removed. In this case, pressure, liquid saturation, permeability in the x -direction, and permeability ratio in the x -direction were removed from the dataset. In addition, features whose values never changed during the numerical simulations were removed as well. Although the correlation coefficient between some independent variables is high, those features were not removed as their individual correlation with some other independent variables is relatively different. The correlation coefficient matrix of the remaining features (independent and dependent variables) is shown in Fig. 4.

The concentrations of K^+ and SO_4^{2-} were negatively correlated to the brittleness index of rocks. The correlations suggest that the higher the concentrations of K^+ and SO_4^{2-} , the lower the brittleness index of the rocks. The distribution of the features is presented in Table 1.

The input features include formation temperature (T in degrees Celsius), gas saturation (SatGas), salt saturation (SatSalt), formation fluid pH, formation water density (Dwat in g/cm^3), ionic strength (IonStr), and the primary aqueous species/ions concentrations (including the amount of dissolved CO₂, in mol/kg H₂O). The unit of concentrations in the table is mol/kg H₂O. The input features (18 variables) are believed to be related to the brittleness index (the output feature). This assumption was made, as the geochemical properties of formation fluid depends on the mineralogical composition of the rock, as the rock minerals are in equilibrium with the formation fluid (Yu et al., 2020; Thanh et al., 2022). Also, the geochemical composition of the formation fluid depends on the in situ temperature conditions of the formation (Ibrahim, 2022). Therefore, the geochemical properties of the formation fluid and the formation temperature might be related to the brittleness index of the formation. The statistical distribution of the overall dataset shows that the mean and median (50th percentile) are different for most of the features. Also, the mean and median of the

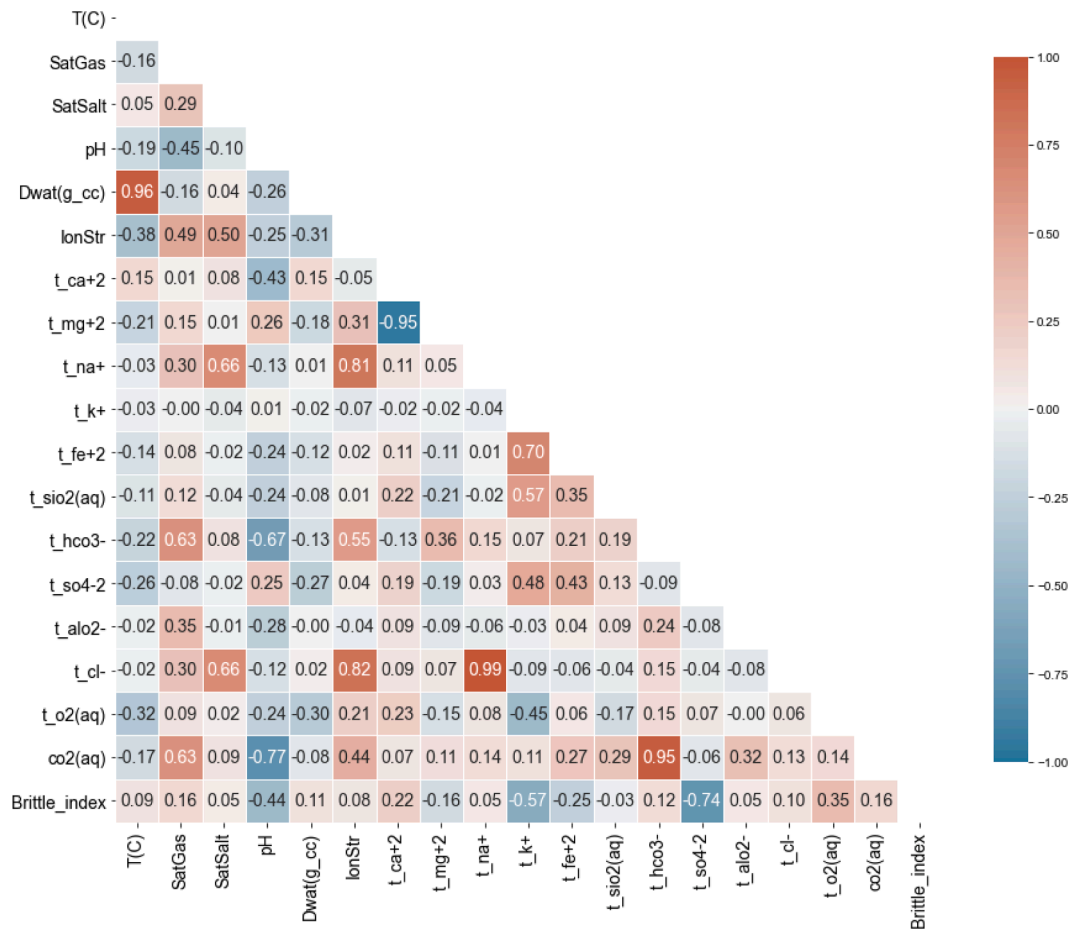


Fig. 4. Correlation coefficient matrix of features.

Table 1
Statistical parameters of the overall dataset.

Variables	Mean	Standard deviation	Minimum	50th percentile	Maximum
T(C)	5.764706e+01	2.733906e+01	4.000000e+01	4.000000e+01	1.000000e+02
SatGas	7.473813e-02	1.608901e-01	0.000000e+00	0.000000e+00	9.818800e-01
SatSalt	5.958950e-04	6.460365e-03	0.000000e+00	0.000000e+00	1.686400e-01
pH	5.740421e+00	1.045728e+00	4.362300e+00	5.649200e+00	7.491000e+00
Dwat(g_cc)	1.062711e+00	3.759167e-02	9.645000e-01	1.043300e+00	1.196900e+00
IonStr	3.281328e+00	1.159284e-01	2.967200e+00	3.271800e+00	4.352500e+00
t_ca+2	3.717171e-01	2.005988e-01	8.954700e-03	4.729800e-01	7.513800e-01
t_mg+2	2.392790e-01	2.509667e-01	9.398500e-02	1.003900e-01	1.004300e+00
t_na+	2.601796e+00	1.076680e-01	2.444800e+00	2.586800e+00	4.051600e+00
t_k+	2.255553e-03	3.771088e-03	1.947900e-11	1.307150e-04	4.134900e-02
t_fe+2	6.208039e-04	2.483182e-03	1.677900e-11	4.252600e-08	2.484400e-02
t_sio2(aq)	1.573913e-03	2.133439e-03	1.948500e-10	2.882450e-04	9.197300e-03
t_hco3-	3.213137e-01	4.268074e-01	6.532200e-05	5.757000e-03	1.346900e+00
t_so4-2	5.747741e-03	5.151247e-03	3.440300e-03	3.642400e-03	4.379000e-02
t_alo2-	1.165757e-08	4.530096e-08	1.288900e-11	1.984900e-10	7.362100e-07
t_cl-	3.740544e+00	1.551220e-01	3.518800e+00	3.723000e+00	5.831600e+00
t_o2(aq)	-2.038282e-07	8.303031e-07	-1.445500e-05	-2.482550e-11	3.260200e-16
co2(aq)	2.465815e-01	3.198288e-01	1.221500e-06	1.974400e-03	8.939000e-01
Brittle_index	3.897865e-01	1.706044e-01	1.070956e-01	5.100000e-01	5.893410e-01

Table 2
Brittleness index distribution in the datasets.

Dataset	Count	Mean	Standard deviation	Minimum	50th percentile	Maximum
Training set	23,990	0.4289	0.1707	0.1071	0.5100	0.5893
Validation set	10,282	0.4288	0.1706	0.1071	0.5100	0.5893
Testing set	3808	0.4299	0.1699	0.1071	0.5100	0.5893

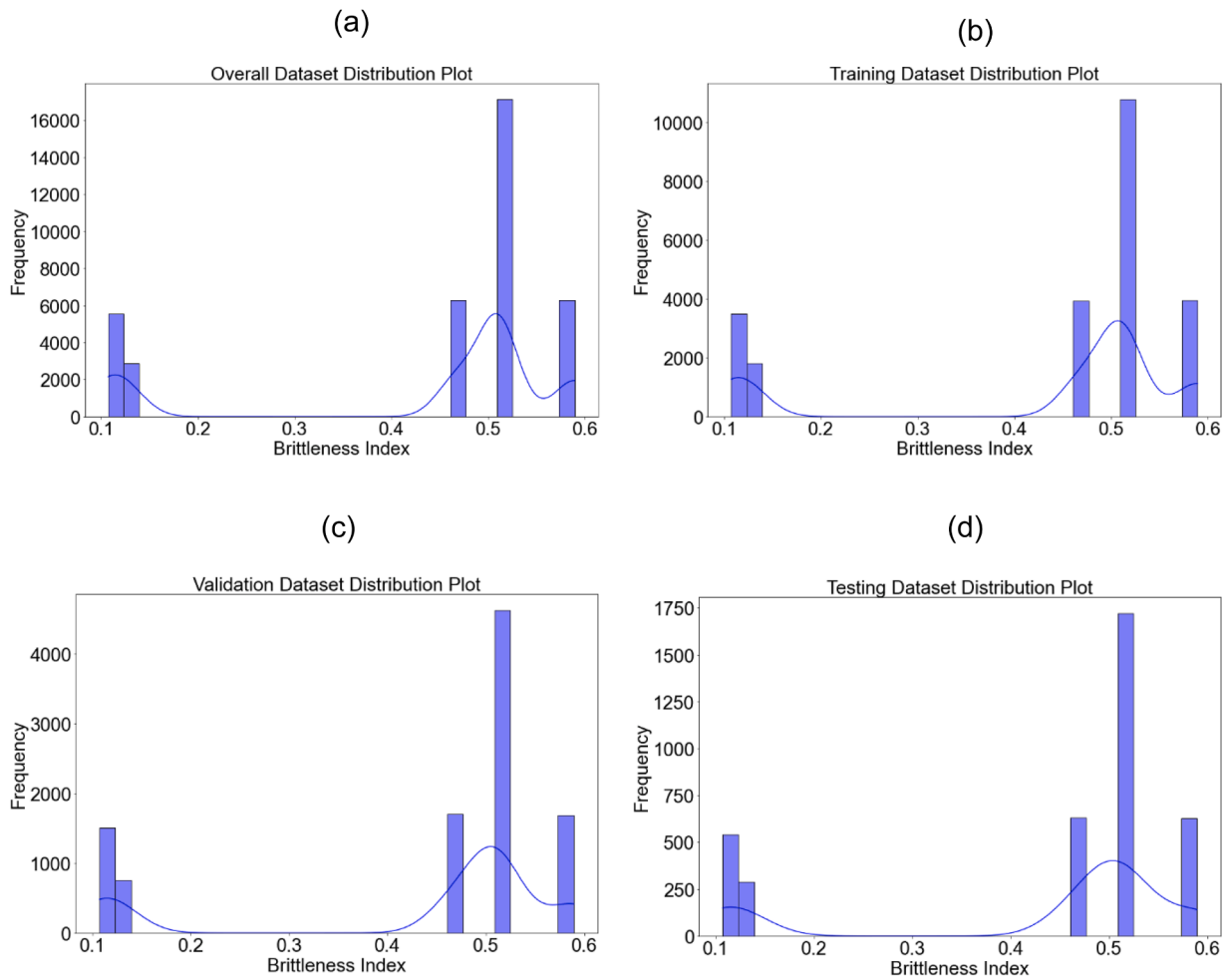


Fig. 5. Brittleness index data distribution.

brittleness index for each of the datasets (training, validation, and testing datasets) are different (Table 2). The data distribution plot (Fig. 5) also shows that the brittleness index appears bimodal in the distribution, forming two clusters of low and high brittleness index, representing the caprock (shale or mud rock) and reservoir rocks (sandstone and carbonate rocks), respectively.

Therefore, the features were scaled. The dependent variable (brittleness index) and independent variables were scaled using a standard scaler, to prevent any input feature with high values from overfitting the model, as other equally important features might be neglected if not scaled. Thus, scaling the features improves the training accuracy (Kannaiah & Maurya, 2023). Standard scaler standardizes the features as follows:

$$z = \frac{x - \mu}{\sigma} \quad (15)$$

where, x represents the input variable, μ and σ are the mean and standard deviation of the variable dataset, respectively.

4.3.2. Model architecture

This study applied the prepared data in developing the machine learning model. The structure of the ANN model is made up of 18 nodes (representing the input parameters) in the input layer, 1–3 hidden layers (each layer has 64 neurons), and a node in the output layer (representing the output parameter – brittleness index). The neural network is fully connected. In each layer (except the output layer), a rectified linear unit (ReLU) was used as an activation function, while a linear activation function was used in the output layer. The ‘He_normal’ weight initializer

was applied (He et al., 2015), as it samples the weights following a normal distribution and a modified standard deviation, taking the number of input neurons for each layer into consideration (Wolfgang et al., 2020).

4.3.3. Model evaluation

To gauge the accuracy of the numerical simulation and machine learning models, some evaluation criteria, including mean absolute error (MAE), mean square error (MSE), mean absolute percentage error (MAPE), and coefficient of determination (R^2 or R-squared score). In the model evaluation, N is the total number of observations (or total number of data values), \hat{y}_i is the predicted i th value, y_i is the actual i th value, and \bar{y} is the mean of actual values.

Mean absolute error (MAE), can be expressed as

$$MAE = \frac{1}{N} \sum_{i=1}^N |y_i - \hat{y}_i| \quad (16)$$

Similarly, the mean square error can be expressed as

$$MSE = \frac{1}{N} \sum_{i=1}^N (y_i - \hat{y}_i)^2 \quad (17)$$

While root-mean-square error (RMSE) is obtained by taking the square root of MSE, and can be expressed as

$$RMSE = \sqrt{\frac{1}{N} \sum_{i=1}^N (y_i - \hat{y}_i)^2} \quad (18)$$

The magnitude of relative error (MRE) for each observation i , and mean magnitude of relative error (MMRE) can be expressed as:

$$\text{MRE}_i = \frac{|y_i - \hat{y}_i|}{y_i} \quad (19)$$

$$\text{MMRE} = \frac{1}{N} \sum_{i=1}^N \text{MRE}_i \quad (20)$$

Mean absolute percentage error (MAPE) is another form of MMRE, but it is expressed in percentage as

$$\text{MAPE} = \frac{1}{N} \sum_{i=1}^N \text{MRE}_i * 100 \quad (21)$$

Coefficient of determination, also called R-squared (R^2) score represents the proportion of the variance in the dependent variable that is predictable from the independent variables (Chicco et al., 2021). It can be expressed as:

$$R^2 = 1 - \frac{\sum_{i=1}^N (y_i - \hat{y}_i)^2}{\sum_{i=1}^N (y_i - \bar{y}_i)^2} \quad (22)$$

4.3.4. ANN model building

To build the artificial neural network model, the prepared dataset made up of 38,080 observations (or rows) and 19 features (18 input features and an output feature) was used in this study. The dataset was divided into three sets: 63 % of the dataset was selected as the training set, 27 % as the validation set, and 10 % as the testing set. The data sets were selected randomly (by setting a random state) to ensure similar data distribution for the training, validation, and testing data sets. The selected proportion of the selected data sets was mainly to have more data to train the model and properly validate the model to avoid overfitting. The training set was used to build the model, while the validation set was employed to ensure the model was not overfitting or underfitting. The testing set was reserved to test the developed and validated model, to ensure there was no form of data leakage during the model development stage, and to reveal the accuracy of the ANN model in estimating brittleness index.

Three options were considered for the model building. The first option has a hidden layer, the second option has 2 hidden layers, while the

third option has 3 hidden layers. Satisfactory tuning of optimizer hyperparameters (the batch size and epochs) of training was performed, using the grid search approach, to obtain better predictions of brittleness index. The batch sizes considered are 32, 64, and 128; while the number of epochs considered are 10, 20, 50, and 100. The loss function and optimizer employed in this study are ‘mean square error’ and ‘Adam’, respectively. During the hyperparameter tuning (or sensitivity analysis), the first option (Option 1), together with a combination of batch size of 32 and 100 epochs, gave the highest mean absolute percentage error of 0.59 % and 0.56 % for the training and validation datasets, respectively (Fig. 6); while the third option (Option 3), together with a combination of batch size of 32 and 100 epochs, gave the lowest mean absolute percentage error of 0.16 % for the training and validation datasets. However, since the mean absolute percentage error for all the options considered is < 1 %, and one of the objectives of the ANN model development is to apply a weight-based approach to generate feature importance using the first hidden layer, Option 1 (with a single hidden layer) was selected for the final ANN model development.

The final ANN model was developed using the predefined architecture and the selected optimal hyperparameters (Option 1), as shown in Table 3. The feature importance of the input parameters was determined

Table 3
Model structure and parameters.

Model Parameters	Option 1	Option 2	Option 3
Number of hidden layers	1	2	3
Number of neurons in each hidden layer	64	64	64
Number of neurons in the output layer	1	1	1
Number of output feature(s)	1	1	1
Number of input features	18	18	18
Activation function in the hidden layers	ReLU	ReLU	ReLU
Kernel initializer	He_normal	He_normal	He_normal
Seed value	42	42	42
Loss function	MSE	MSE	MSE
Optimizer	Adam	Adam	Adam
Learning rate	Default	Default	Default
Best batch size	32	32	32
Best number of epochs	100	100	100
Model Performance			
MAPE on the train dataset (%)	0.57	0.16	0.16
MAPE on the validation dataset (%)	0.59	0.17	0.16

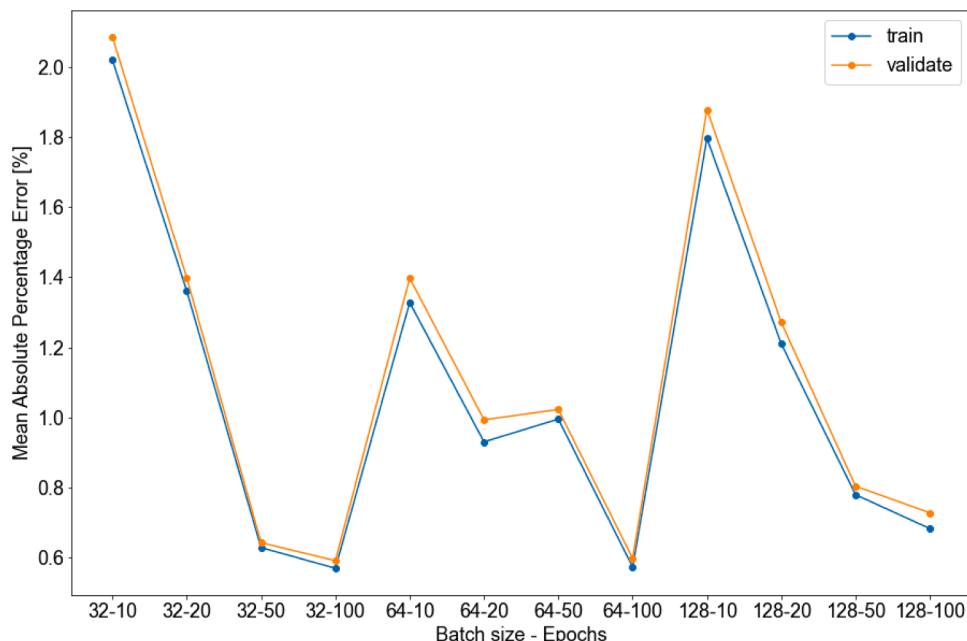


Fig. 6. Sensitivity analysis of model performance based on batch size and epochs.

by comparing the sum of the absolute weights (in the first hidden layer) of each parameter that predicted the brittleness index and was ranked in order. This technique helps to understand the relative importance of different input features in predicting the brittleness index.

4.3.5. Model validation

Data utilized in the development of the machine learning model is from the work of Aminaho (2024). The predicted brittleness index, using the ANN model developed in this study, was validated with the actual brittleness index (calculated by incorporating molecular weight and molar volume of minerals, and their volume fractions from numerical simulations performed by Aminaho (2024) into the mathematical model derived by Aminaho and Hossain (2023)). In other words, the ANN model was validated with the brittleness index in the testing dataset, and the performance of the ANN model was evaluated.

Furthermore, to validate the feature importance generated using the ANN model, an Extreme Gradient Boosting (XGBoost) model was also developed in this study (Chen & Guestrin, 2016). XGBoost has powerful software-level optimizations and can handle imbalanced data through weighting (Wiens et al., 2025). The hyperparameters selected for the XGBoost model training include gamma (0.0, 0.1, 0.2, 0.3), maximum depth of tree (5, 6, 8, 10), learning rate (0.01, 0.05, 0.10, 0.15), and number of estimators (20, 50, 100, 150). The optimal hyperparameters selected using a grid search approach on a 10-fold cross-validation of the scaled training dataset for the XGBoost model are gamma (0.0), maximum depth (5), learning rate (0.15), and number of estimators (150).

4.4. Limitations of the study

Only two temperature conditions (40 °C and 100 °C) were considered in this study. Using several temperature conditions could have given more insight into the changes in brittleness index of rocks as formation temperature changes during CO₂ geosequestration. Also, the numerical simulation data used as a case study in the machine learning model development in the present study were not validated with experimental or field data, but they were compared using relevant experimental data from previous studies. The brittleness index calculations based on data from the numerical simulations could not be validated using data from rock core sample experiments, as some portion of the fluids injected into the reservoir (in the numerical simulations) migrated to the caprock. Therefore, field data would have been more suitable to validate such numerical simulations. However, no field data with such simulation cases was available at the time of the study. Hence, the machine learning model developed in the present study was based only on the post-processing stage of the numerical simulation dataset. Therefore, the machine learning model developed in the present study was not validated with field data, but with unseen data (from the numerical simulation post-processed data) reserved for the ANN model testing. To develop a more reliable machine learning model that can be applied in CO₂ storage fields in different parts of the world, it is vital to apply the complete algorithm developed in the present study.

5. Results and discussion

To investigate the performance of the ANN model in predicting brittleness of rocks, the data set was divided into a training set (63 %), a

validation set (27 %), and a testing set (10 %). The testing set was reserved to avoid data leakage and measure the performance of the model. The computed analysis of the final ANN model is shown in Table 4. The R² value is over 99.92 %, MAPE is <0.59 %, MAE is <0.002, and RMSE is about 0.005. The performance of the model on all the data sets is similar, indicating that the model is not overfitting. Thus, the model predicts the brittleness index of rocks with high accuracy.

The XGBoost model developed in this study also performs well, with R² value of over 94.16 %, MAPE is <5.89 %, MAE is <0.020, and RMSE is about 0.04 (Table 5). However, the ANN model performed better than the XGBoost model in this study.

The predicted brittleness index based on the ANN model (using the testing data set) is plotted against the actual brittleness index (R² = 1.0) as shown in Fig. 7. The brittleness index basically formed two clusters: low (indicating shale rocks) and high (indicating carbonate or sandstone rocks).

The ANN model developed in the present study predicts the brittleness index of the formations with an R² value greater than 99 % and a Mean Absolute Percentage Error (MAPE) of <0.6 %. Therefore, the ANN model predicts the brittleness index of the formations with high accuracy. The model performance is in consonance with other applications of the ANN model in previous studies. The performance of the ANN model developed by Ibrahim (2022) to predict coal wettability during CO₂ geosequestration in coal-water-CO₂ system is high, with MAPE <7 %. Also, the performance of the ANN model developed by Tillerio (2024) to predict the effectiveness of CO₂ trapping in deep saline aquifers is high, with an R² value of at least 95 %. The significantly higher performance of the ANN model in the present study might be attributed to very few cases of CO₂ geosequestration, rock/fluid properties, and operating conditions considered while performing the numerical simulations.

The significance of the input features (independent variables) in the ANN model developed in this study, referred to as feature importance, was evaluated based on the sum of the absolute weights of each input feature in the neurons of the first hidden layer (in the final model). The features with a higher sum of absolute weights were assumed to contribute more to the final predictions of the ANN model. The significance of the input features in predicting brittleness index using the final ANN model is shown in Fig. 8. Based on the ANN model, SiO₂ (aq), SO₄²⁻, K⁺, Ca²⁺, O₂ (aq), pH, formation temperature (T), and Mg²⁺ are the more important factors affecting the brittleness index prediction, while salt saturation least affected the brittleness index of the formations.

To validate the weight-based feature importance generated using ANN model, feature importance was generated using the XGBoost model as shown in Fig. 9. Based on the XGBoost model, SO₄²⁻, K⁺, Ca²⁺, O₂ (aq), Cl⁻, and SiO₂ (aq), are the more important factors affecting the brittleness index prediction, while salt saturation least affected the brittleness index of the formations.

Comparing the ANN and XGBoost models, the more important features include SiO₂ (aq) concentration, SO₄²⁻ concentration, K⁺ concentration, Ca²⁺ concentration, and O₂ (aq) concentration. These features significantly impact the brittleness of rocks as they reflect the mineral composition of the formations and redox reactions that influence the brittleness index of rocks. For instance, high SO₄²⁻ concentration relates to the volume fraction of anhydrite (Hedayati et al. 2018), which negatively correlated ($r = -0.74$) with the brittleness index in this study; Ca²⁺ concentration relates to calcite and dolomite minerals; SiO₂ (aq) concentration relates to quartz and other silicon oxide-based minerals;

Table 4
Performance measurements of the final ANN model.

Data set	Performance measures			
	R ²	MAPE (%)	MAE	RMSE
Training set (63 %)	0.999311	0.563577	0.001804	0.004482
Validation set (27 %)	0.999253	0.585620	0.001842	0.004662
Testing set (10 %)	0.999449	0.551608	0.001720	0.002084

Table 5
Performance measurements of the XGBoost model.

Data set	Performance measures			
	R ²	MAPE (%)	MAE	RMSE
Training set (63 %)	0.999996	0.072954	0.000139	0.000325
Validation set (27 %)	0.990956	2.468275	0.004700	0.016226
Testing set (10 %)	0.941519	5.884240	0.019013	0.041083

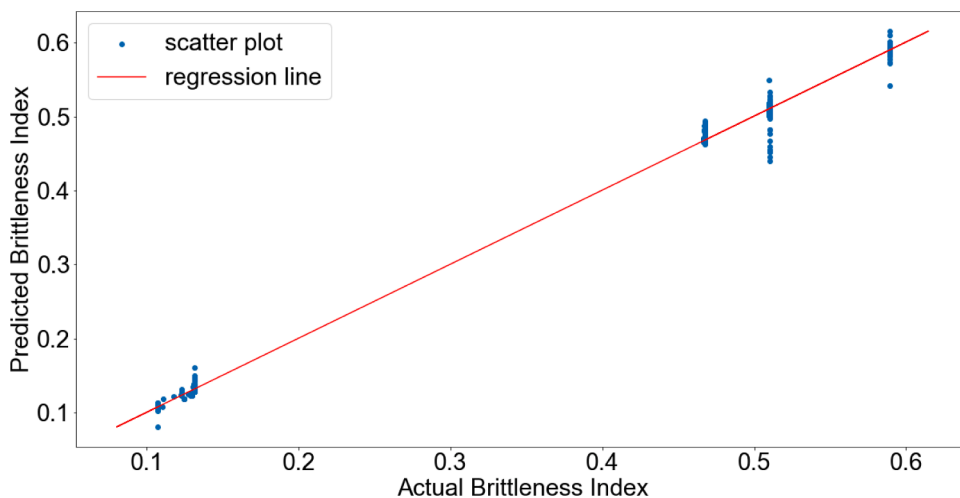


Fig. 7. A plot of predicted and actual brittleness index from the testing data set based on ANN model.

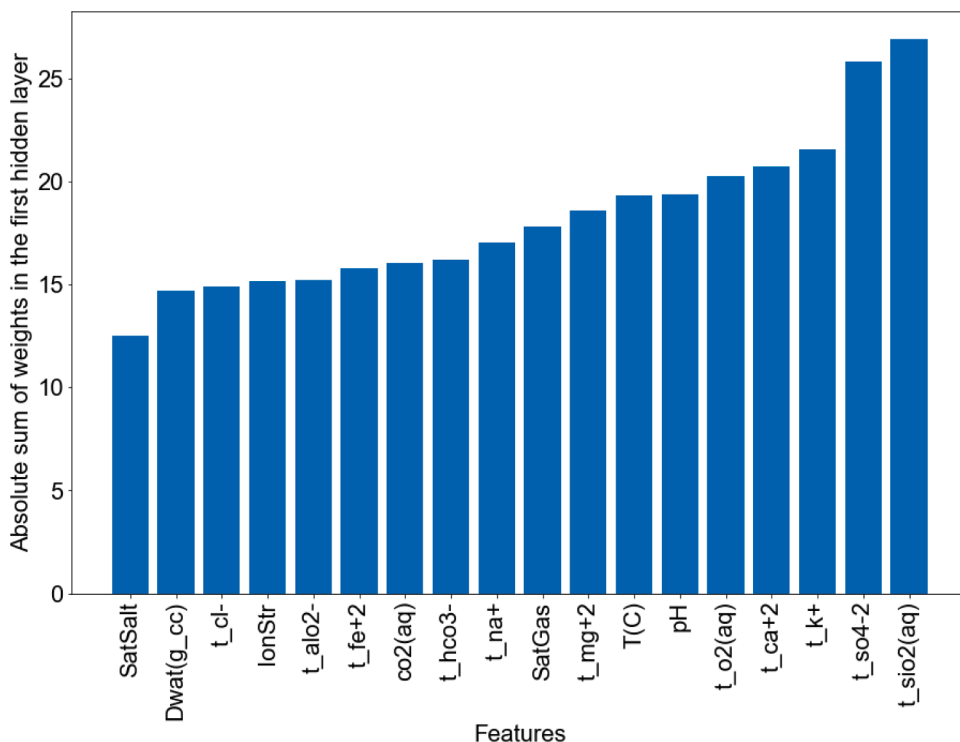


Fig. 8. Feature importance using the final ANN model.

and K^+ concentration relates to K-feldspar and illite. Therefore, the geochemical composition of the formation fluid is the main factor that impacts the prediction of the brittleness index of the formation using a machine learning model. The dissolution of one mineral might result in the precipitation of another mineral having a common ion. For example, the dissolution of dolomite might result in the precipitation of calcite (having Ca^{2+} as a common ion). Therefore, proper training of the machine learning model makes it possible for the model to learn the concentration changes (as well as their rates of change) as some minerals dissolve or precipitate during CO_2 geosequestration, and the resulting change in the brittleness of the formation.

6. Conclusions

In this study, an algorithm for the generation of numerical simulation

datasets for reliable machine learning model development was developed, and an ANN model was developed to evaluate the brittleness of reservoir (sandstone and carbonate) and cap (shale) rocks before and during CO_2 geosequestration. Based on the key findings in this study, the conclusions from predicting brittleness index of rocks using the machine learning model developed are summarized as follows:

1. In terms of feature importance in predicting the brittleness index of rocks, the concentrations of $SiO_2(aq)$, SO_4^{2-} , K^+ , Ca^{2+} , and $O_2(aq)$ have a stronger impact in the prediction of brittleness of rocks considered in the present study. High SiO_2 concentration could suggest the presence of highly brittle minerals, such as quartz, in the rock. In contrast, higher SO_4^{2-} concentration could suggest lower brittleness. Higher SO_4^{2-} concentration could also signify the presence of less brittle (low brittleness index) minerals, such as anhydrite or

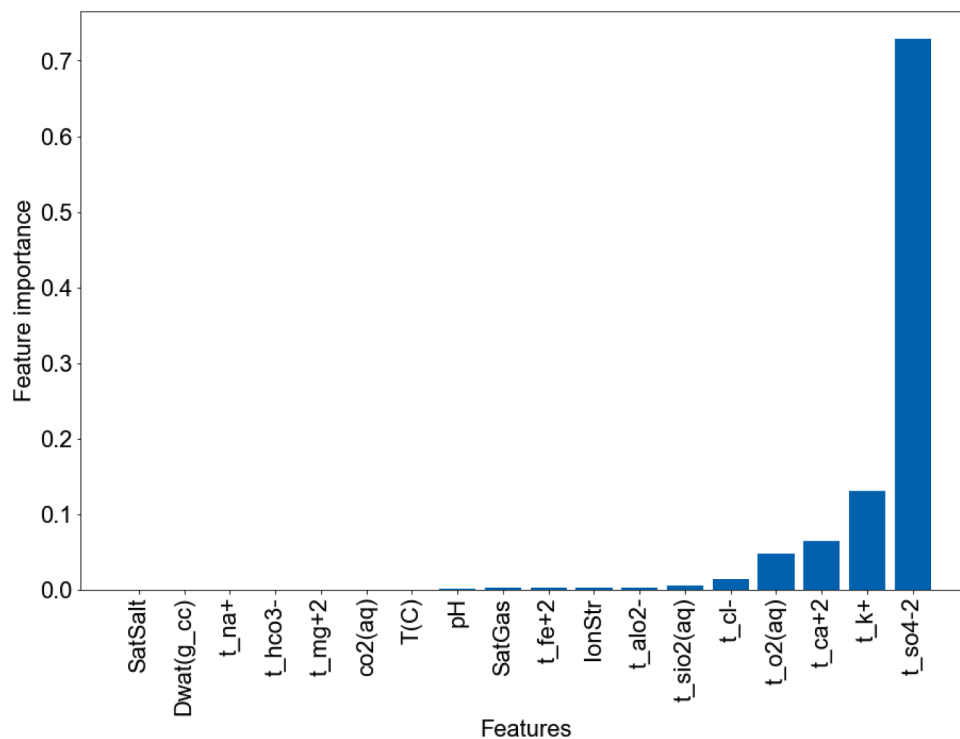


Fig. 9. Feature importance using the XGBoost model.

promote the precipitation of such minerals. Besides, oxidation of pyrite in the presence of water can increase SO_4^{2-} concentration. So, for formations that have pyrite as one of their primary minerals, its oxidation could increase SO_4^{2-} concentration.

- Formation fluid geochemical compositions and formation temperature are important parameters in predicting the brittleness index of rocks, while the amount of dissolved CO_2 in formation water has little or no effect on the brittleness index of rocks. It appears that what matters in terms of the amount of CO_2 is that CO_2 gas dissolves in the formation water up to the amount required to enable fluid-rock chemical reaction or mineral trapping. Other extra amounts of dissolved CO_2 subsequently during the period of storage might not impact the brittleness of the rocks over the geosequestration period considered (100 years).
- The ANN model predicted the brittleness index of rocks with R^2 value greater than 99 %, indicating that over 99 % of the variance in the brittleness index is predicted by the model; and mean absolute percentage error (MAPE) < 0.6 % on the training, validation, and testing data sets. Thus, the ANN model predicts the brittleness index of rocks with very high accuracy.
- The algorithm developed to process numerical simulation data will help in the development of a more robust and reliable machine learning model, which can be applied in different CO_2 storage sites or fields for the evaluation of the brittleness index of formations. The algorithm can also be applied to any engineering problem to develop highly accurate machine learning models.

7. Recommendations for future study

- Future studies should consider developing mathematical models to evaluate the brittleness of rocks by incorporating formation fluid chemical composition, formation temperature, and other important parameters that relate to dissolution and precipitation of minerals.
- A larger range of data from several numerical simulations (with similar software) with their corresponding calculated brittleness index should be utilized in developing similar machine learning

models to obtain a more generalized and universally acceptable model for rock brittleness index prediction.

- Future study should apply the complete algorithm developed in this study or use numerical simulation datasets that have passed through the complete processing stages proposed in the algorithm, to develop a more reliable machine learning model to evaluate the brittleness index of rocks before and during CO_2 geosequestration.

Author credit statement

Efenwengbe Nicholas Aminaho: Conceptualization, Investigation, Project Administration, Methodology, Modelling, Validation, Analyses, and Writing-Original Draft and Review. **Mamdud Hossain:** Writing-Review. Supervisor. **Nadimul Haque Faisal:** Supervisor. **Reza San-ae:** Supervisor.

Declaration of competing interest

The authors declare that they have no known competing financial interests or personal relationships that could have appeared to influence the work reported in this paper.

Acknowledgements

The authors would like to acknowledge the flexible funding and partnership offered by the UK Carbon Capture and Storage Research Centre (UKCCSRC). This project was jointly funded by the Robert Gordon University (Aberdeen) and UKCCSRC.

Data availability

Data will be made available on request.

References

Aminaho, E. N. (2024). *Caprock integrity evaluation for geosequestration of CO_2 in depleted petroleum reservoirs*. Robert Gordon University. PhD thesis.

- Aminaho, E. N., & Hossain, M. (2023). *Caprock integrity evaluation for geosequestration of CO₂ in low-temperature reservoirs*. Aberdeen: Robert Gordon University. <https://rgu-repository.worktribe.com/output/2072081>.
- Alam, M. M., Hjuler, M. L., Christensen, H. F., & Fabricius, I. L. (2014). Petrophysical and rock-mechanics effects of CO₂ injection for enhanced oil recovery: Experimental study on chalk from South Arne field, North Sea. *Journal of Petroleum Science and Engineering*, 122, 468–487.
- AL-Ameri, W. A., Abdulraheem, A., Mahmoud, M., Abdullatif, O., & Adebayo, A. R. (2014). Effect of CO₂ sequestration period on the mechanical properties of carbonate aquifers. In *Paper SPE 171702-MS presented at the Abu Dhabi International Petroleum Exhibition and Conference held in Abu Dhabi, UAE, 10–13 November 2014*. <https://doi.org/10.2118/171702-MS>
- AL-Ameri, W. A., Abdulraheem, A., & Mahmoud, M. (2016). Long-term effects of CO₂ sequestration on rock mechanical properties. *Journal of Energy Resources Technology*, 138(1), Article 012201. <https://doi.org/10.1115/1.4032011>. Article.
- Bachu, S. (2002). Sequestration of CO₂ in geological media in response to climate change: Road map for site selection using the transform of the geological space into the CO₂ phase space. *Energy Conversion and Management*, 43, 87–102.
- Cao, C., Liao, J., Hou, Z., Wang, G., Feng, W., & Fang, Y. (2020). Parametric uncertainty analysis for CO₂ sequestration based on distance correlation and support vector regression. *Journal of Natural Gas Science and Engineering*, 77, Article 103237. <https://doi.org/10.1016/j.jngse.2020.103237>. Article.
- Chen, B., Harp, D. R., Lin, Y., Keating, E. H., & Pawar, R. J. (2018). Geologic CO₂ sequestration monitoring design: A machine learning and uncertainty quantification based approach. *Applied Energy*, 225, 332–345.
- Chen, T., & Guestrin, C. (2016). XGBoost: A scalable tree boosting system. In *Proceedings of the 22nd ACM SIGKDD International Conference on Knowledge Discovery and Data Mining* (pp. 785–794). <https://doi.org/10.1145/2939672.2939785>
- Chicco, D., Warrens, M. J., & Jurman, G. (2021). The coefficient of determination R-squared is more informative than SMAPE, MAE, MAPE, MSE and RMSE in regression analysis evaluation. *PeerJ Computer Science*, 7, 623. <https://doi.org/10.7717/peerj-cs.623>
- Elwegaa, K., Emadi, H., Soliman, M., Gamadi, T., & Elsharafi, M. (2019). Improving oil recovery from shale oil reservoirs using cyclic cold carbon dioxide injection – An experimental study. *Fuel*, 254, Article 115586. <https://doi.org/10.1016/j.fuel.2019.05.169>. Article.
- Ezema, I. C., Edelugo, S. O., Menon, A. R. R., & Omah, A. D. (2015). A comparative prediction of the tensile properties of sisal Fiber reinforced epoxy composite using volume fraction and mass fraction models. *Journal of Metallurgical and Materials Engineering Research*, 1(2), 9–18.
- Ghorayeb, K., Mogensen, K., El Droubi, N., Kloucha, C. K., & Mustapha, H. (2024). Physics-enhanced machine-learning-based prediction of fluid properties for gas injection – Focus on CO₂ injection. *Gas Science and Engineering*, 123, Article 205228. <https://doi.org/10.1016/j.jgsce.2024.205228>. Article.
- Harati, S., Gomari, S. R., Rahman, M. A., Hassan, R., Hassan, I., Sleiti, A. K., & Hamilton, M. (2024). Performance analysis of various machine learning algorithms for CO₂ leak prediction and characterization in geo-sequestration injection wells. *Process Safety and Environmental Protection*, 183, 99–110.
- He, K., Zhang, X., Ren, S., & Sun, J. (2015). Delving deep into rectifiers: Surpassing human-level performance on imagenet classification. Paper presented at IEEE International Conference on Computer Vision held in Santiago, Chile, 7-13 December 2015, 1026–1034. <https://doi.org/10.1109/ICCV.2015.123>.
- He, Y., Zhou, Y., Wen, T., Zhang, S., Huang, F., Zou, X., Ma, X., & Zhu, Y. Q. (2022). A review of machine learning in geochemistry and cosmochemistry: Method improvements and applications. *Applied Geochemistry*, 140, 1–13. <https://doi.org/10.1016/j.apgeochem.2022.105273>
- Hedayati, M., Wigston, A., Wolf, J. L., Rebscher, D., & Niemi, A. (2018). Impacts of SO₂ gas impurity within a CO₂ stream on reservoir rock of a CCS pilot site: Experimental and modelling approach. *International Journal of Greenhouse Gas Control*, 70, 32–44. <https://doi.org/10.1016/j.jggc.2018.01.003>
- Heidari, M., Ajalloeian, R., Ghazifard, A., & Isfahanian, M. H. (2020). Evaluation of P and S wave velocities and their return energy of rock specimen at various lateral and axial stresses. *Geotech Geol Eng*, 38, 3253–3270.
- Hood, S. B., Cracknell, M. J., & Gazley, M. F. (2018). Linking protolith rocks to altered equivalents by combining unsupervised and supervised machine learning. *Journal of Geochemical Exploration*, 186, 270–280.
- Hou, B., Zeng, Y., Fan, M., & Li, D. (2018). Brittleness evaluation of shale based on the Brazilian splitting test. *Geofluids*, 2018, Article 3602852. <https://doi.org/10.1155/2018/3602852>. Article.
- Huang, Y.-H., Yang, S.-Q., Hall, M. R., & Zhang, Y.-C. (2018). The effects of NaCl concentration and confining pressure on mechanical and acoustic behaviors of brine-saturated sandstone. *Energies*, 11(2), 385. <https://doi.org/10.3390/en11020385>
- Huang, Y.-H., Yang, S.-Q., Li, W.-P., & Hall, M. R. (2020). Influence of SuperCritical CO₂ on the strength and fracture behavior of BrineSaturated sandstone specimens. *Rock Mechanics and Rock Engineering*, 53, 653–670.
- Hucka, V., & Das, B. (1974). Brittleness determination of rocks by different methods. *International Journal of Rock Mechanics and Mining Sciences & Geomechanics*, 11, 389–392.
- Ibrahim, A. F. (2023). Prediction of shale wettability using different machine learning techniques for the application of CO₂ sequestration. *International Journal of Coal Geology*, 276, Article 104318. <https://doi.org/10.1016/j.coal.2023.104318>. Article.
- Ibrahim, A. F. (2022). Prediction of coal wettability using machine learning for the application of CO₂ sequestration. *International Journal of Greenhouse Gas Control*, 118, Article 103670. <https://doi.org/10.1016/j.jggc.2022.103670>. Article.
- Jijo, B. T., & Abdulazeez, A. M. (2021). Classification based on decision tree algorithm for machine learning. *Journal of Applied Science and Technology Trends*, 2(1), 20–28.
- Kang, Y., Shang, C., Zhou, H., Huang, Y., Zhao, Q., Deng, Z., Wang, H., & Ma, Y. Z. (2020). Mineralogical brittleness index as a function of weighting brittle minerals—From laboratory tests to case study. *Journal of Natural Gas Science and Engineering*, 77, Article 103278. <https://doi.org/10.1016/j.jngse.2020.103278>. Article.
- Kannaiah, P. V. D., & Maurya, N. K. (2023). Machine learning approaches for formation matrix volume prediction from well logs: Insights and lessons learned. *Geoenvironment Science and Engineering*, 229, Article 212086. <https://doi.org/10.1016/j.geoen.2023.212086>. Article.
- Klovov, A., Treviño, R. H., & Meckel, T. A. (2017). Diffraction imaging for seal evaluation using ultra high resolution 3D seismic data. *Marine and Petroleum Geology*, 82, 85–96.
- Kolawole, O., Assaad, R. H., Adams, M. P., Ngoma, M. C., Anya, A., & Assaf, G. (2023). Coupled experimental assessment and machine learning prediction of mechanical integrity of MICP and cement paste as underground plugging materials. *Biogeotechnics*, 1(2), Article 100020. <https://doi.org/10.1016/j.bgtech.2023.100020>. Article.
- Li, H. (2022). Research progress on evaluation methods and factors influencing shale brittleness: A review. *Energy Reports*, 8, 4344–4358.
- Li, S., Zhang, S., Xing, H., & Zou, Y. (2022). CO₂-brine-rock interactions altering the mineralogical, physical, and mechanical properties of carbonate-rich shale oil reservoirs. *Energy*, 256, Article 124608. <https://doi.org/10.1016/j.energy.2022.124608>. Article.
- Liu, M., Bai, B., & Li, X. (2014). Experimental studies on the short term effect of CO₂ on the tensile failure of sandstone. *Energy Procedia*, 63, 3357–3363.
- Liu, Y., Ma, T., Wu, H., & Chen, P. (2020). Investigation on mechanical behaviors of shale cap rock for geological energy storage by linking macroscopic to mesoscopic failures. *Journal of Energy Storage*, 29, Article 101326. <https://doi.org/10.1016/j.est.2020.101326>. Article.
- Lyu, Q., Long, X., Ranjith, P. G., Tan, J., Kang, Y., & Luo, W. (2018). A damage constitutive model for the effects of CO₂-brine-rock interactions on the brittleness of a low-clay shale. *Geofluids*, 2018, Article 7321961. <https://doi.org/10.1155/2018/7321961>. Article.
- Masoudi, R., Jaili, M. A. A., Press, D. J., Lee, K.-H., Tan, C. P., Anis, L., Darman, N. B., & Othman, M. (2011). An integrated reservoir simulation-geomechanical study on feasibility of CO₂ storage in M4 Carbonate reservoir, Malaysia. In *Paper IPTC 15029 presented at the International Petroleum Technology Conference held in Bangkok, Thailand, 15-17 November 2011*.
- Mavhengere, P., Wagner, N., & Malumbazo, N. (2022). Influences of SO₂ contamination in long term supercritical CO₂ treatment on the physical and structural characteristics of the Zululand Basin caprock and reservoir core samples. *Journal of Petroleum Science and Engineering*, 215, Article 110554. <https://doi.org/10.1016/j.petrol.2022.110554>. Article.
- McNaughton, B.A.P. (2019). Two-dimensional ising spin model and machine learning. <https://doi.org/10.13140/RG.2.2.33154.43201>.
- Meng, F., Zhou, H., Zhang, C., Xu, R., & Lu, J. (2015). Evaluation methodology of brittleness of rock based on post-peak stress-strain curves. *Rock mechanics and rock engineering*, 48, 1787–1805.
- Mouallem, J., Raza, A., Glatz, G., Mahmoud, M., & Arif, M. (2024). Estimation of CO₂-brine interfacial tension using machine Learning: Implications for CO₂ geo-storage. *Journal of Molecular Liquids*, 393, Article 123672. <https://doi.org/10.1016/j.molliq.2023.123672>. Article.
- Nyakilla, E. E., Jun, G., Kasimu, N. A., Robert, E. F., Innocent, N., Mohamedy, T., Shaame, M., Ngata, M. R., & Mabeyo, P. E. (2022). Application of machine learning in the prediction of compressive and shear strengths from the experimental data in oil well cement at 80 °C: Ensemble trees boosting approach. *Construction and Building Materials*, 317(4), Article 125778. <https://doi.org/10.1016/j.conbuildmat.2021.125778>. Article.
- Pan, B., Song, T., Yue, M., Chen, S., Zhang, L., Edlmann, K., Neil, C. W., Zhu, W., & Iglauer, S. (2024). Machine learning-based shale wettability prediction: Implications for H₂, CH₄ and CO₂ geo-storage. *International Journal of Hydrogen Energy*, 56, 1384–1390.
- Panfilov, M., et al. (2016). Underground and pipeline hydrogen storage. In B. Ram, et al. (Eds.), *Compendium of Hydrogen Energy*, 2 pp. 91–115). Woodhead Publishing. <https://doi.org/10.1016/B978-1-78242-362-1.00004-3>.
- Pearce, J. K., Kirste, D. M., Dawson, G. K. W., Rudolph, V., & Golding, S. D. (2019). Geochemical modelling of experimental O₂-SO₂-CO₂ reactions of reservoir, cap-rock, and overlying cores. *Applied Geochemistry*, 109, Article 104400. <https://doi.org/10.1016/j.apgeochem.2019.104400>. Article.
- Punnam, P. R., Dutta, A., Krishnamurthy, B., & Surasani, V. K. (2023). Study on utilization of machine learning techniques for geological CO₂ sequestration simulations. *Materials Today: Proceedings*, 72, 378–385.
- Rashidi, S., Mohamadani, N., Ghorbani, H., Wood, D. A., Shahbazi, K., & Alvar, M. A. (2020). Shear modulus prediction of embedded pressurized salt layers and pinpointing zones at risk of casing collapse in oil and gas wells. *Journal of Applied Geophysics*, 183, Article 104205. <https://doi.org/10.1016/j.jappgeo.2020.104205>. Article.
- Tariq, Z., Ali, M., Hassanpouryouzband, A., Yan, B., Sun, S., & Hoteit, H. (2023). Predicting wettability of mineral/CO₂-brine systems via data-driven machine learning modeling: Implications for carbon geo-sequestration. *Chemosphere*, 345, Article 140469. <https://doi.org/10.1016/j.chemosphere.2023.140469>. Article.
- Tariq, Z., Abdulraheem, A., Elkhatatny, S., Mahmoud, M., Muqtadir, A., & Murtaza, M. (2018). Geomechanical studies on CO₂ sequestered rocks in an aqueous saline environment. In *Paper SPE 192242-MS presented at the Annual Technical Symposium & Exhibition held in Dammam, Saudi Arabia, 23–25 April 2018*.

- Thanh, H. V., & Lee, K.-K. (2022). Application of machine learning to predict CO₂ trapping performance in deep saline aquifers. *Energy*, 239, Article 122457. <https://doi.org/10.1016/j.energy.2021.122457>. Article.
- Thanh, H. V., Yasin, Q., Al-Mudhafar, W. J., & Lee, K.-K. (2022). Knowledge-based machine learning techniques for accurate prediction of CO₂ storage performance in underground saline aquifers. *Applied Energy*, 314, Article 118985. <https://doi.org/10.1016/j.apenergy.2022.118985>. Article.
- Tillero, E. (2024). Machine learning-based modelling for geologic CO₂ storage in deep saline aquifers. Case study of bunter sandstone in Southern North Sea. *International Journal of Greenhouse Gas Control*, 133, Article 104077. <https://doi.org/10.1016/j.ijggc.2024.104077>. Article.
- Wang, H., Williams-Stroud, S., Crandall, D., & Chen, C. (2024). Machine learning and deep learning for mineralogy interpretation and CO₂ saturation estimation in geological carbon storage: A case study in the Illinois Basin. *Fuel*, 361, Article 130586. <https://doi.org/10.1016/j.fuel.2023.130586>. Article.
- Wang, Y., Zhang, X., & Liu, X. (2021). Machine learning approaches to rock fracture mechanics problems: Mode-I fracture toughness determination. *Engineering Fracture Mechanics*, 253, Article 107890. <https://doi.org/10.1016/j.engfracmech.2021.107890>. Article.
- Wei, X. C., Li, Q., Li, X.-Y., Sun, Y.-K., & Liu, X. H. (2015). Uncertainty analysis of impact indicators for the integrity of combined caprock during CO₂ geosequestration. *Engineering Geology*, 196, 37–46.
- Wiens, M., Verone-Boyle, A., Henscheid, N., Podichetty, J. T., & Burton, J. (2025). A tutorial and use case example of the eXtreme gradient boosting (XGBoost) artificial intelligence algorithm for drug development applications. *Clinical and Translational Science*, 18(3), Article e70172. <https://doi.org/10.1111/cts.70172>. Article.
- Wolfgang, M., Weißensteiner, M., Clarke, P., Hsiao, W.-K., & Khinast, J. G. (2020). Deep convolutional neural networks: Outperforming established algorithms in the evaluation of industrial optical coherence tomography (OCT) images of pharmaceutical coatings. *International Journal of Pharmaceutics*, X, 2, Article 100058. <https://doi.org/10.1016/j.ijpx.2020.100058>
- Wu, H., Lubbers, N., Viswanathan, H. S., & Pollyea, R. M. (2021). A multi-dimensional parametric study of variability in multi-phase flow dynamics during geologic CO₂ sequestration accelerated with machine learning. *Applied Energy*, 287, Article 116580. <https://doi.org/10.1016/j.apenergy.2021.116580>. Article.
- Xu, T., Sonnenthal, E., Spycher, N., & Zheng, L. (2014). TOUGHREACT V3.0-OMP reference Manual: A parallel simulation program for non-isothermal multiphase geochemical reactive transport.
- Yang, Y., Ju, B.-S., Lü, G.-Z., & Huang, Y. (2024). Machine learning methods for predicting CO₂ solubility in hydrocarbons. *Petroleum Science*, 21(5), 3340–3349. <https://doi.org/10.1016/j.petsci.2024.04.018>
- Yao, P., Yu, Z., Zhang, Y., & Xu, T. (2023). Application of machine learning in carbon capture and storage: An in-depth insight from the perspective of geoscience. *Fuel*, 333(1), Article 126296. <https://doi.org/10.1016/j.fuel.2022.126296>. Article.
- Yu, H., Wang, Z., Rezaee, R., Zhang, Y., Nwider, L. N., Liu, X., Verrall, M., & Iglauer, S. (2020). Formation water geochemistry for carbonate reservoirs in Ordos basin, China: Implications for hydrocarbon preservation by machine learning. *Journal of Petroleum Science and Engineering*, 185, Article 106673. <https://doi.org/10.1016/j.petrol.2019.106673>. Article.
- Zhang, W., Xu, T., & Li, Y. (2011). Modeling of fate and transport of coinjection of H₂S with CO₂ in deep saline formations. *Journal of Geophysical Research*, 116, Article B02202. <https://doi.org/10.1029/2010JB007652>. Article.